Nuclear Physics B344 (1990) 207–237
North-Holland

PHASE DIAGRAM OF A LATTICE SU(2) ⊗ SU(2) SCALAR-FERMION MODEL WITH NAIVE AND WILSON FERMIONS*

Wolfgang BOCK[1,2], Asit K. DE[1,2], Karl JANSEN[2], Jiří JERSÁK[1,2], Thomas NEUHAUS[3] and Jan SMIT[4]

[1]*Institut für Theoretische Physik E, RWTH Aachen, D-5100 Aachen, FRG*
[2]*HLRZ c/o KFA Jülich, P.O. Box 1913, D-5170 Jülich, FRG*
[3]*Fakultät für Physik, Universität Bielefeld, D-4800 Bielefeld, FRG*
[4]*Institute of Theoretical Physics, Valckenierstraat 65, NL-1018 XE Amsterdam, The Netherlands*

Received 26 March 1990

We present the phase structure of the chiral $SU(2)_L \otimes SU(2)_R$ scalar-fermion model on the lattice with on-site Yukawa coupling y and Wilson–Yukawa coupling w for positive y and w. The hopping parameter κ of the four-component scalar field of fixed length is both positive and negative. From the different behaviour of several observables ferromagnetic, paramagnetic and antiferromagnetic phases can be distinguished. They split into different regions or phases with small and large $y + 4w$. A similar structure is also found in the quenched approximation. In addition, in the unquenched case a ferrimagnetic phase is found at negative κ around $y + 4w \approx \sqrt{2}$. We discuss fermion masses in various regions and point out the possibilities of decoupling the unwanted fermion doublers in the continuum limit in analogy to the Wilson mechanism.

1. Introduction

Recent years have witnessed a lot of interest in the nonperturbative understanding of the symmetry breaking sector of the standard model of electroweak interactions. Many of these studies concentrated on the pure scalar sector regularized on a lattice, neglecting gauge and fermion fields (for references see the recent reviews [1, 2]). Whereas it is presumably sufficient to treat the gauge fields only perturbatively, the inclusion of fermions into the nonperturbative investigation is important because of the possibility that some heavy fermions exist with strong Yukawa interactions. Keeping the perturbative triviality of the Yukawa coupling in mind, it is of phenomenological importance to investigate a possible upper limit on the fermion mass generated through this coupling and to improve the already existing upper limit on the Higgs mass, now with fermionic feedback included. Alternatively, any indication that strong Yukawa coupling might lead to a nontriv-

*Supported by the Deutsches Bundesministerium für Forschung und Technologie, by the Deutsche Forschungsgemeinschaft and by the Stichting voor Fundamenteel Onderzoek der Materie (FOM).

ial fixed point with an interacting symmetry breaking sector would be of major interest for the standard model and, more generally, for quantum field theory.

Field-theoretically it is a challenge to regularize a theory with chirally coupled fermions on the lattice. The problem is due to the well-known "species doubling" of lattice fermions, which results for chiral theories also in the occurrence of chiral doublers or "mirror" fermions [3]. It is nontrivial to remove these unwanted doublers by the Wilson mechanism [4].

Many of the initial investigations of coupled scalar-fermion models (for reviews see refs. [2,5–7]) have temporarily avoided the problem of fermion doubling and explored qualitative properties of models with strong Yukawa coupling. They have looked at scalar-fermion theories on the lattice with Z(2), U(1) and SU(2) symmetries using naive lattice fermions or staggered fermions with either on-site or hypercubic Yukawa coupling [7–18]. The information on phase diagrams has been obtained from a combination of approximate analytic calculations and numerical simulations and is not yet complete. Nevertheless, the following universal features seem to come out from these exploratory studies of models with on-site Yukawa couplings:

(i) Within the broken symmetry phase with a nonvanishing expectation value v of the scalar field (ferromagnetic phase) there is a weak Yukawa coupling region where the standard perturbative analysis applies. In addition there is also a nonperturbative strong Yukawa coupling region in which the fermion masses *increase* as v decreases at a constant Yukawa coupling [12–16, 19].

(ii) Investigations with dynamical fermions [9–14, 17, 18] demonstrate that intermediate values of the Yukawa coupling strongly favour a ferromagnetic ordering of the scalar fields. The broken symmetry phase extends to negative values of the hopping parameter κ for the scalar field. Thus at least for such Yukawa couplings the region of negative κ could well be of interest for taking the continuum limit.

(iii) For intermediate values of the Yukawa coupling the phase diagram for negative κ has a very complicated structure, as several phases come close together [10, 12]. Analytic studies performed until now [14, 17] fail to describe this region even qualitatively.

Because of fermion doubling all the above models are vector-like, their spectrum is unsatisfactory from the phenomenological point of view and some modifications are required. Several proposals modifying or extending the Wilson mechanism (see, e.g. ref. [20]) have been discussed recently in ref. [6].

A very promising possibility is to introduce, in addition to the usual Yukawa coupling of strength y, another Yukawa-like coupling term, the Wilson–Yukawa coupling of strength w, having the character of the Wilson term [5, 6, 21–23]. However, due to the presence of the scalar field, this coupling maintains the chiral symmetry manifestly and the doublers acquire heavy masses dynamically. To see whether the doublers get decoupled in the scaling region, leaving a chiral scalar-fermion theory applicable in the continuum, one naturally needs a nonperturbative

treatment of the model even if the mass of the remaining physical fermion is assumed to be small. A mean field calculation [19] and simulations in a U(1) ⊗ U(1) model [24] gave very promising results in this respect.

We have recently made a numerical investigation of the chiral $SU(2)_L \otimes SU(2)_R$ model [12,25] on the lattice with the Wilson–Yukawa term in the broken phase and have shown, in the quenched approximation, that for relatively large and fixed values of w the fermion doublers can indeed be given masses of the order of the increasing cut-off as the critical region is approached, while the physical fermion mass can have arbitrarily small values. For the Wilson–Yukawa mechanism of chiral lattice fermions to hold, our conclusions from the quenched approximation have to carry over to the full model with dynamical fermions.

In this paper we therefore continue our investigation of the chiral $SU(2)_L \otimes SU(2)_R$ scalar-fermion model, including now the fermion dynamics. The first important aim is to determine the phase structure of the model and to localize the regions of physical interest. Even keeping the quartic scalar field coupling infinite (the length of the four-component scalar field is fixed to unity) we have a system with three coupling parameters κ, y and w. We have investigated systematically this three-dimensional space for $y, w \geqslant 0$ and arbitrary real κ. We have found seven different phases or distinctly different phase regions. Some phases, or different regions of one phase, have the same symmetries but are distinguished by the combined strength of the two Yukawa couplings. Roughly, for $y + 4w \ll \sqrt{2}$ the model has *weak Yukawa coupling* phases or regions, where the perturbative analysis in y and w is applicable. For example, in the ferromagnetic phase the fermion and the doubler masses decrease with the decreasing vacuum expectation value v of the scalar field. In contrary, in the *strong Yukawa coupling* regions found for $y + 4w \gg \sqrt{2}$ the Yukawa couplings have a distinctly nonperturbative character and in particular the fermion and the doubler masses increase with decreasing v at fixed y and w [19,25].

We show in fig. 1 the phase structure of the full model with two doublets of dynamical fermions for the $w = 0$ case. This phase diagram in a preliminary form was shown earlier [12]. It is qualitatively similar to the phase structure found recently in the U(1) model [10]. For $w > 0$ the phase diagram remains the same as that for $w = 0$ except that the funnel-like structure in fig. 1 around $y \approx \sqrt{2}$ shifts to the left with increasing w and is found around $y \approx \sqrt{2} - 4w$ until it disappears from the half-plane $y \geqslant 0$. We use the following notation for the phases and regions we have found:

Symmetric phases:

PMW: Paramagnetic phase with weak Yukawa couplings

PMS: Paramagnetic phase with strong Yukawa couplings

Broken symmetry phases and their regions:

FM(W): Ferromagnetic phase (weak Yukawa coupling region)

FM(S): Ferromagnetic phase (strong Yukawa coupling region)

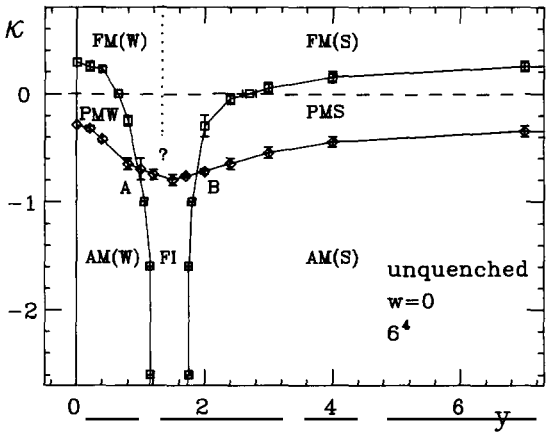

Fig. 1. Phase diagram for $w = 0$ in the unquenched case. A and B are probably two quadruple points where four phases meet. The approximate position of the crossover in the FM phase is indicated by the dotted line.

AM(W): Antiferromagnetic phase (weak Yukawa coupling region)
AM(S): Antiferromagnetic phase (strong Yukawa coupling region)
FI: Ferrimagnetic phase.

We cannot completely rule out the possibility that the AM(W) and AM(S) regions are separated for arbitrarily large negative κ by the funnel containing the FI phase. This phase is less and less distinguishable as κ decreases and we could not locate its end. Thus we cannot exclude that it continues until $\kappa = -\infty$.

For $w = 0$ the various phase transition lines meet, within our precision of their localization, in two quadruple points (points A and B in fig. 1). In the three-dimensional phase diagram these points become lines which we call lines A, B.

Fig. 2 shows the phase diagram for the same model at $w = 0$ in the quenched approximation. The dotted and the dashed lines denote a crossover, across which the behaviour of various observables with the fermionic fields changes significantly. For finite w its position shifts to $y \approx \sqrt{2} - 4w$. For weak and strong Yukawa couplings $y + 4w$ the unquenched phase diagram is very similar to the quenched one. The diagrams differ significantly in the region $y + 4w \approx \sqrt{2}$. When fermion loops are included the dashed part of the crossover in the quenched case develops, approximately at the same position, into the funnel filled with the FI phase. We expect that the width of the funnel grows with the number of dynamical fermion species. With the exception of the FI phase all the phases and regions of the phase diagram with dynamical fermions have analogues in the quenched case.

The outline of the paper is as follows: The model, its symmetries, its fermion content and the most important observables are described in sect. 2. In sect. 3 we summarize the presently available analytic information on the phase structure and

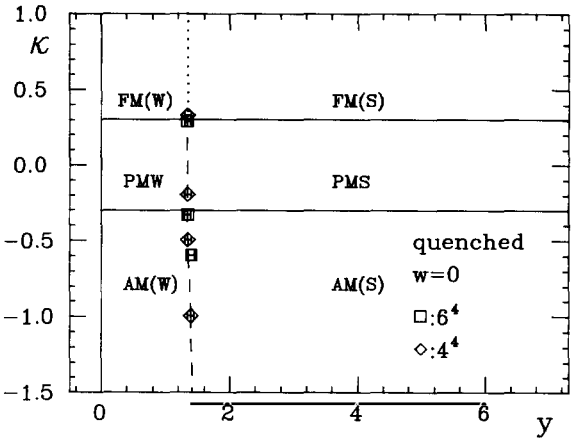

Fig. 2. Phase diagram for $w = 0$ in the quenched case. The crossover in the FM phase is again indicated by the dotted line. Its continuation in the PM and AM phase is indicated by the dashed line.

on the behaviour of some observables. In sect. 4 we describe the results obtained in the quenched approximation for the behaviour of several observables in the three-dimensional parameter space. It provides us with a useful guideline for an understanding of the different phases found in the full model, and of the phase transitions. In sect. 5 we establish for the unquenched model the different phases, the phase regions and the phase transitions in the y–κ plane at $w = 0$ and describe the dependence of the phase structure on w for $w > 0$. We conclude and discuss possible physical relevance of various regions of the phase diagram in sect. 6.

2. The model

2.1. THE ACTION AND ITS SYMMETRIES

The model is given on the euclidean lattice by the action $S = S_H + S_F$, with

$$S_H = -\kappa \sum_{x\mu} \tfrac{1}{2} \mathrm{Tr}\left(\Phi_x^\dagger \Phi_{x+\hat{\mu}} + \Phi_{x+\hat{\mu}}^\dagger \Phi_x\right), \tag{2.1}$$

$$\begin{aligned} S_F = {} & \sum_{x\mu} \tfrac{1}{2}\left(\overline{\Psi}_x \gamma_\mu \Psi_{x+\hat{\mu}} - \overline{\Psi}_{x+\hat{\mu}} \gamma_\mu \Psi_x\right) + y \sum_x \overline{\Psi}_x \left(\Phi_x P_R + \Phi_x^\dagger P_L\right) \Psi_x \\ & + w \sum_{x\mu} \Big\{ \overline{\Psi}_x \left(\Phi_x P_R + \Phi_x^\dagger P_L\right) \Psi_x - \tfrac{1}{2}\Big[\overline{\Psi}_x \left(\Phi_x P_R + \Phi_{x+\hat{\mu}}^\dagger P_L\right) \Psi_{x+\hat{\mu}} \\ & + \overline{\Psi}_{x+\hat{\mu}} \left(\Phi_{x+\hat{\mu}} P_R + \Phi_x^\dagger P_L\right) \Psi_x \Big] \Big\}. \end{aligned} \tag{2.2}$$

The scalar field Φ_x is a 2×2 SU(2) matrix. The freezing of the radial mode corresponds to the choice of infinite bare quartic coupling of the scalar field. The experience from the pure Φ^4 theory suggests that such a model belongs to the same universality class as models with finite quartic coupling. The fermion fields Ψ_x and $\overline{\Psi}_x$ are SU(2) doublets, κ is the hopping parameter for the scalar field, y is the usual Yukawa coupling, w is the Wilson–Yukawa coupling* and $P_{\mathrm{L,R}}$ are left- and right-handed chiral projectors.

The action is invariant under the global chiral $\mathrm{SU(2)_L} \otimes \mathrm{SU(2)_R}$ transformations

$$\Psi_x \to (\Omega_{\mathrm{L}} P_{\mathrm{L}} + \Omega_{\mathrm{R}} P_{\mathrm{R}}) \Psi_x , \tag{2.3}$$

$$\overline{\Psi}_x \to \overline{\Psi}_x (\Omega_{\mathrm{L}}^{\dagger} P_{\mathrm{R}} + \Omega_{\mathrm{R}}^{\dagger} P_{\mathrm{L}}) , \tag{2.4}$$

$$\Phi_x \to \Omega_{\mathrm{L}} \Phi_x \Omega_{\mathrm{R}}^{\dagger} , \tag{2.5}$$

where $\Omega_{\mathrm{L,R}} \in \mathrm{SU(2)_{L,R}}$. In the context of the standard model the $\mathrm{SU(2)_L}$ symmetry changes into the local gauge symmetry and the global $\mathrm{SU(2)_R}$ symmetry is broken to an extent required by the mass differences within the weak isodoublets.

For $w = 0$ there are the usual staggered fermion symmetries (see, e.g. [26]), extended in obvious fashion to the scalar field. We mention also the chiral $\mathrm{U(4)_L} \otimes \mathrm{U(4)_R}$ symmetry [27] present for $y = w = 0$, which is most easily expressed in the staggered representation

$$\chi_x \to \exp(i\gamma + i\varepsilon_x \gamma') \chi_x ,$$

$$\overline{\chi}_x \to \overline{\chi}_x \exp(-i\gamma + i\varepsilon_x \gamma') , \tag{2.6}$$

$$\varepsilon_x = (-1)^{x_1 + x_2 + x_3 + x_4} , \tag{2.7}$$

where

$$\chi_x = T_x \Psi_x , \qquad \overline{\chi}_x = \overline{\Psi}_x T_x^{\dagger} ,$$

$$T_x = \gamma_1^{x_1} \ldots \gamma_4^{x_4} , \tag{2.8}$$

and γ and γ' are arbitrary 4×4 matrices built from the Dirac γ-matrices.

For $w = 0$ the model has furthermore the discrete LR symmetry

$$P_{\mathrm{L,R}} \Psi_x \to P_{\mathrm{R,L}} \Psi_x , \qquad \overline{\Psi}_x P_{\mathrm{R,L}} \to \overline{\Psi}_x P_{\mathrm{L,R}} , \qquad \Phi_x \to \Phi_x^{\dagger} , \tag{2.9}$$

which is broken for $w \neq 0$.

* The parameters y, w are related to r, M used in refs. [5, 6, 19, 22] by $w = r$, $y = M - 4r$.

For $y = 0$ the model also has the global symmetry

$$P_R \Psi_x \to P_R \Psi_x + \epsilon, \qquad P_R \overline{\Psi}_x \to P_R \overline{\Psi}_x + \bar{\epsilon}, \tag{2.10}$$

which guarantees that the fermion mass m'_F is zero and also that the right-handed fermion in the standard model decouples at $y = 0$ for $\kappa \to \kappa_c$ and any w [28]. Note that one expects in a symmetric phase for $w > 0$ in general two distinct fermion masses m_F and m'_F corresponding to fermion fields transforming respectively as $SU(2)_L \otimes \mathbb{1}_R$ and $\mathbb{1}_L \otimes SU(2)_R$, whereas in the FM phase $m_F = m'_F$ [6, 19]. For $w = 0$, $m_F = m'_F$ always holds, because of the LR symmetry (2.9) (assuming it is not dynamically broken).

For the purpose of an understanding of the phase diagram it is also useful to notice at $y = w = 0$ an invariance of the action with respect to the standard staggered field transformation

$$\kappa \to -\kappa, \qquad \Phi_x \to \varepsilon_x \Phi_x. \tag{2.11}$$

This invariance can be extended for $w = 0$ to $y \neq 0$ [17] by also transforming the fermion fields

$$(\Psi_x, \overline{\Psi}_x) \to \exp(\tfrac{1}{4} i \varepsilon_x \pi)(\Psi_x, \overline{\Psi}_x), \tag{2.12}$$

and making the on-site Yukawa coupling y purely imaginary,

$$y \to -iy. \tag{2.13}$$

This can be interpreted as a remnant of the staggered chiral U(1) transformation. For $w \neq 0$ this invariance is violated by the one-link part of the Wilson term in eq. (2.2).

Finally, we mention the invariance

$$\Phi_x \to -\Phi_x, \qquad y \to -y, \qquad w \to -w. \tag{2.14}$$

It means that without loss of generality one can restrict the study of the phase diagram to half of the y, w plane. We constrain our study to $y, w \geqslant 0$, however.

The motivation [21–23] for the inclusion of the manifestly invariant Wilson–Yukawa coupling is the wish to give the doubler fermions masses of the order of the cutoff and to decouple them in the scaling region.

Recall that for the free inverse Wilson fermion propagator (we use lattice units with the lattice constant $a = 1$)

$$S_0^{-1}(p) = i \sum_\mu \gamma_\mu s_\mu + m + r \sum_\mu (1 - c_\mu), \tag{2.15}$$

where

$$s_\mu = \sin p_\mu , \qquad c_\mu = \cos p_\mu , \tag{2.16}$$

the fermion masses are given by

$$m_n = (m + 2n) . \tag{2.17}$$

Here n is the number of momentum components p_μ equal to π, with $n = 0$ for the physical fermion mass m and $n = 1$–4 for the doubler masses which remain of order of the cutoff in the continuum limit. The Wilson–Yukawa coupling term in eq. (2.2) is expected to increase the mass of the doublers in a similar way, now, however, by means of a dynamical process which has to be treated nonperturbatively [5, 6, 22].

The fermion determinant of the model is real because of the pseudoreality of the SU(2) group, but not necessarily positive. To guarantee its positivity, required for the Hybrid Monte Carlo algorithm [29] we are using, we introduce implicitly two replicas of the fermionic fields by squaring the determinant. It is also known in the continuum gauge theory that an even number of $SU(2)_L$ doublets is required [30]. The identical doublets in our simulation have the same chiral couplings and we thus avoid an explicit introduction of mirror fermions.

2.2. OBSERVABLES

To investigate the complex phase structure of the model it is necessary to look simultaneously at several observables. Here we list the definitions of some useful observables on a lattice of finite volume V. As the exact definitions of the observables are quite involved, we also introduce some short-hand mnemotechnic notation for them.

Magnetization:

$$\langle \Phi \rangle \mathbb{1} = v \mathbb{1} = \left\langle \frac{1}{V} \sum_x \Phi_x \right\rangle \Bigg|_{\text{rot}} . \tag{2.18}$$

The index "rot" means that each configuration of the scalar field Φ_x obtained during the Monte Carlo simulation is rotated in the $O(4) \simeq SU(2)_L \otimes SU(2)_R/Z(2)$ symmetry space so that

$$\frac{1}{V} \sum_x \Phi_x = M \mathbb{1} \tag{2.19}$$

is proportional to the unit matrix. Thus $\langle \Phi \rangle = \langle M \rangle$. This procedure, used in the simulations of the pure Φ^4 models [31], compensates for the drift of the system on finite lattices through the set of degenerate ground states in a phase with broken

symmetry. This drift would cause the vanishing of an observable noninvariant with respect to the symmetry transformations (2.3)–(2.5) even if its expectation value in the thermodynamic limit is nonzero. Recently it has been demonstrated that the rotation provides a very good approximation to the infinite volume quantities [32].
Staggered magnetization:

$$\langle \Phi_{\mathrm{st}} \rangle \mathbb{1} = v_{\mathrm{st}} \mathbb{1} = \left\langle \frac{1}{V} \sum_x \varepsilon_x \Phi_x \right\rangle \Bigg|_{\mathrm{rot}} . \tag{2.20}$$

Also here a rotation for each configuration is performed so that the quantity $\Sigma_x \varepsilon_x \Phi_x$ is proportional to $\mathbb{1}$. This rotation is in general not identical with that leading to eq. (2.19). It is therefore possible that on finite lattices $v + v_{\mathrm{st}} > 1$ (as happens for some of our data).
Link product:

$$\langle \Phi^\dagger U \Phi \rangle = z^2 = \left\langle \frac{1}{8V} \sum_{x,\mu} \mathrm{Tr}\, \Phi_x^\dagger \Phi_{x+\hat{\mu}} \right\rangle . \tag{2.21}$$

This observable is invariant with respect to the transformations (2.3)–(2.5). Here U in the mnemotechnic notation stands for the link separating the Φ's. In a gauge theory U would be a link variable.
Fermion condensate:

$$\langle \overline{\Psi} \Psi \rangle = - \left\langle \frac{1}{8V} \sum_x \overline{\Psi}_x \Psi_x \right\rangle \Bigg|_{\mathrm{rot}} . \tag{2.22}$$

The rotation leading to eq. (2.19) is performed on the scalar field before the quantity $\langle \overline{\Psi} \Psi \rangle$ is calculated by the fermion matrix inversion.
Invariant fermion condensate:

$$\langle \overline{\Psi} \Phi \Psi \rangle = - \left\langle \frac{1}{8V} \sum_x \overline{\Psi}_x \left(\Phi_x^\dagger P_{\mathrm{L}} + \Phi_x P_{\mathrm{R}} \right) \Psi_x \right\rangle . \tag{2.23}$$

This observable is proportional to the Yukawa term in the action (2.2).

As expected, the noninvariant quantities are much more sensitive to the phase transitions between phases of different symmetry than the invariant ones. This is due to their role as order parameters. On the other hand, $\langle \overline{\Psi} \Phi \Psi \rangle$ can distinguish different regions of the same symmetry. We have also monitored the invariant observables for the reason that if the gauge fields were included these observables would become gauge invariant, whereas the others would vanish identically by the

Elitzur theorem. Thus gaining experience with the invariant observables is useful for later purposes.

In addition to the listed observables we use the available information on the fermion and the doubler masses, obtained mainly in refs. [12, 16, 25] for the FM phase in the quenched approximation and now in the same way also for the PM phase at $w = 0$.

Furthermore, we have found it very useful to monitor in all our runs the number of conjugate gradient iterations N_{CG} required for the inversion, with a given accuracy, of the fermion matrix. This quantity is sensitive to the presence of small eigenvalues of the fermion matrix [33].

3. Some analytical considerations of the phase structure

Some of the information collected in this section has been obtained for models which are analogous to but not the same as our model with $w = 0$. However, we expect that Yukawa models with different symmetry groups but with on-site Yukawa coupling have very similar phase structure and that the results obtained there carry over to our model, at least qualitatively. In addition we present some mean field analysis for $w > 0$.

3.1. LIMITING CASES OF YUKAWA COUPLINGS

We first summarize the available information on our model for vanishing or very strong Yukawa couplings.

$y = 0$, $w = 0$. In this limit the fermions are massless and free. Thus the well-known [31, 34] phase structure of the pure O(4)-symmetric Φ^4 theory (2.1) at infinite quartic coupling is obtained. One critical point is at $\kappa = \kappa_c = 0.3045(7)$. It separates the ferromagnetic phase FM(W) ($\kappa > \kappa_c$) from the paramagnetic phase PMW at $-\kappa_c < \kappa < \kappa_c$ (cf. fig. 2). A second phase transition at $\kappa = -\kappa_c$ is related through the symmetry (2.11) to that at $\kappa = \kappa_c$. For $\kappa < -\kappa_c$ the model is in the antiferromagnetic phase AM(W). The order parameters distinguishing these three phases are $\langle \Phi \rangle$, which is nonvanishing in the FM(W) phase, and $\langle \Phi_{st} \rangle$ having nonzero values in the AM(W) phase.

$y \to \infty$, $w \geqslant 0$. If the on-site Yukawa coupling gets large, the rescaling of the fermion field $\Psi \to 1/\sqrt{y}\,\Psi$ suppresses both the fermion kinetic term and the Wilson–Yukawa term in the action (2.2). As these are the only terms coupling the fermion fields on different lattice sites, the fermions cannot propagate, their masses get infinite and the fermions thus decouple. The phase diagram is that of the pure Φ^4 model. For the scalar field of fixed length it is the same model as at $y = 0$, because the fermion determinant depends on the length of the scalar field

only. The phases are those with the strong Yukawa couplings: FM(S) ($\kappa > \kappa_c$), PMS ($|\kappa| < \kappa_c$) and AM(S) ($\kappa < -\kappa_c$).

$y = 0$, $w > 0$. As follows from ref. [28] the fermion mass m'_F must stay at zero.

3.2. WEAK AND STRONG YUKAWA COUPLING REGIONS

Recently it has been realized [12, 14–16, 19, 25] that for strong Yukawa coupling the relationship between the fermion mass and v in the FM(S) phase is quite different from that in perturbation theory. The existence of two regions of Yukawa couplings can be understood by means of a simple consideration: In the weak coupling region the Yukawa couplings are relatively small and perturbation in w, y is appropriate, giving $m \approx yv$ and $r \approx wv$ in eq. (2.15). Since $v \to 0$ as $\kappa \searrow \kappa_c$, in the weak coupling region $m, r \to 0$. Deep in the strong coupling region the Yukawa couplings are relatively large and the hopping expansion for the fermion propagator can be used [15, 19]. It leads to $m \approx yz^{-1}$ and $r \approx wz^{-1}$ [19]. Since z decreases as $\kappa \searrow \kappa_c$, the fermion masses increase. We note that $z = z_c \approx 0.44 \neq 0$ at $\kappa = \kappa_c$ so that the fermion masses stay finite on the critical line.

Furthermore, the fermion masses stay nonzero for large Yukawa coupling also in the PMS phase [14, 19], though $v = 0$ there. On the other hand, for small Yukawa couplings the fermion masses vanish in the PMW phase [14]. These results for the fermion mass imply the existence of two paramagnetic phases. At the moment we do not see whether in our model one can define a fermion mass in the AM phase because of the staggered structure of the scalar fields. The recently obtained [35] result showing that in the model with staggered fermions and hypercubic Yukawa coupling the fermion mass vanishes in the AM phase for any y does not carry over to our case*.

3.3. MEAN FIELD ESTIMATES OF THE PHASE DIAGRAM

The phase structure of several lattice Yukawa models similar to our model at $w = 0$ has been recently investigated with the mean field method in refs. [13, 14, 17–19]. We expect that the results hold qualitatively also in our case and do not repeat these analyses. The phase diagram is reasonably well described for $y \ll \sqrt{2}$ and $y \gg \sqrt{2}$ and it becomes clear that the FM phase continues to negative κ. However, for $y \approx \sqrt{2}$ at negative κ the mean field results obtained until now do not reproduce the phase structure found in numerical simulations in ref. [10] and in this work. In particular, the FI phase has not been detected.

To get a rough idea about the problems of the mean field method in the region $y \approx \sqrt{2}$ and $\kappa < 0$ we have carried out, similar to ref. [19], a simple mean field calculation in the saddle point formulation both in the weak and the strong Yukawa coupling regions with the following ansatz for the scalar field and for the

* We thank R.E. Shrock for correspondence on this point.

mean field H:

$$\Phi_x = (v + \varepsilon_x v_{\mathrm{st}})\,\mathbb{1}\,, \qquad H_x = (h + \varepsilon_x h_{\mathrm{st}})\,\mathbb{1}\,, \tag{3.1}$$

where v, v_{st}, h and h_{st} are real. In the leading order, neglecting fluctuations completely, this method does not produce the FI phase. Otherwise it gives results qualitatively consistent with our numerical simulations. It also indicates that for $w > 0$ the phase diagram in the y–κ plane is very similar to that at $w = 0$ except a shift along the lines $y + 4w = \mathrm{const}$. In the remainder of this subsection we show some quantitative results of these calculations.

In the weak Yukawa coupling region with $w = 0$, the mean field equations lead to the following estimates for the critical κ as functions of y:

$$\kappa_{\mathrm{c}} \sim \pm\tfrac{1}{4} - \frac{n}{2} y^2 \int_{-\pi/2}^{\pi/2} \frac{\mathrm{d}^4 p}{\pi^4} \frac{1}{s^2} = \pm 0.25 - 0.62 y^2\,, \tag{3.2}$$

respectively, for the FM(W)–PMW and AM(W)–PMW transitions. Here

$$s^2 = \sum_{\mu} s_{\mu}^2\,, \tag{3.3}$$

and n is the number of fermion doublets (i.e. $n = 2$ in our hybrid Monte Carlo calculation). The two transition lines given by eq. (3.2) do not cross each other anywhere. Also, there exists no solution with simultaneous nonzero values of v and v_{st}. Thus, at least in the leading approximation, the FI phase is missing.

The mean field results in the strong coupling region with $w = 0$ are similar. FM(S)–PMS and AM(S)–PMS transition lines again do not intersect and the FI phase does not appear.

The strong coupling mean field calculations can be done easily also with $w > 0$. The mean field equations are given by

$$\begin{aligned} hv &= 4\kappa v^2 + 2nv^2 \int_{-\pi}^{\pi} \frac{\mathrm{d}^4 p}{(2\pi)^4} \frac{s^2}{s^2\left(v^2 - v_{\mathrm{st}}^2\right) + \mathscr{M}^2}\,, \\ hv_{\mathrm{st}} &= -4\kappa v_{\mathrm{st}}^2 - 2nv_{\mathrm{st}}^2 \int_{-\pi}^{\pi} \frac{\mathrm{d}^4 p}{(2\pi)^4} \frac{s^2}{s^2\left(v^2 - v_{\mathrm{st}}^2\right) + \mathscr{M}^2}\,, \end{aligned} \tag{3.4}$$

$$\begin{aligned} 8v &= W'(h + h_{\mathrm{st}}) + W'(h - h_{\mathrm{st}})\,, \\ 8v_{\mathrm{st}} &= W'(h + h_{\mathrm{st}}) - W'(h - h_{\mathrm{st}})\,, \end{aligned} \tag{3.5}$$

where $W(h) = \ln \int \mathrm{d}V \exp \mathrm{Tr}(H^\dagger V + V^\dagger H)$ with $H = H^\dagger = h\mathbb{1}$ is the familiar group integral over the group elements V. Primes represent derivatives and $\mathscr{M} = y + w\sum_\mu (1 - c_\mu)$. With $v_{\mathrm{st}} = 0$ the first of these equations gives eq. (9) of ref. [19] after the replacement $\kappa \to 2\kappa$.

The FM(S)–PMS boundary can be approached from within the FM(S) phase ($v_{\mathrm{st}} = 0$) by letting $v \to 0$ ($h \to v$). The first of the above equations then reduces to

$$v^2 = 4\kappa_c v^2 + 2nv^2 \int_{-\pi}^{\pi} \frac{\mathrm{d}^4 p}{(2\pi)^4} \frac{s^2}{\mathscr{M}^2} . \tag{3.6}$$

One can have a reasonable approximation to the above integral by simply replacing each of c_μ and s_μ by their average values, i.e. taking $s^2 = 2$ and $\mathscr{M} = y + 4w$, which leads to

$$\kappa_c \approx \tfrac{1}{4} - \frac{n}{(y + 4w)^2} . \tag{3.7}$$

Similarly the AM(S)–PMS transition is given by

$$\kappa_c \approx -\tfrac{1}{4} - \frac{n}{(y + 4w)^2} . \tag{3.8}$$

The transition lines again do not intersect, and we find no FI solution with $v \neq 0$ and $v_{\mathrm{st}} \neq 0$ simultaneously. Interestingly, as the w coupling is turned on, the above two formulas suggest a shift of the phase diagram along the lines $y + 4w = \mathrm{const.}$, i.e. the way we observe in our numerical simulation. We also note that the critical points for $y = \infty$ or $w = \infty$ are equal to those of the pure Φ^4 theory in the mean field approximation.

3.4. $\kappa \to +\infty$ LIMIT

In this limit the action for the scalar field (2.1) makes the scalar field constant. With $\Phi_x = \mathbb{1}$ the fermions become free with the propagator (2.15) where $m = y$ and $r = w$. Further information is obtained by considering the eigenvalues $\mu + i\lambda$ of the fermion matrix

$$(\mu, \lambda) = \left(y + 4w - w\sum_\mu c_\mu, \pm \sqrt{\sum_\mu s_\mu^2} \right), \tag{3.9}$$

which determine the fermion condensate $\langle \overline{\Psi}\Psi \rangle$,

$$\langle \overline{\Psi}\Psi \rangle = \frac{1}{8V} \sum \frac{\mu}{\mu^2 + \lambda^2} . \tag{3.10}$$

Here the sum extends over all eigenvalues.

The form of $\langle \overline{\Psi}\Psi \rangle$ as a function of y and w can be estimated by replacing each c_μ and s_μ^2 in eq. (3.9) by their average values, i.e.

$$(\mu, \lambda) \to (y + 4w, \pm\sqrt{2}), \tag{3.11}$$

which gives

$$\langle \overline{\Psi}\Psi \rangle \simeq \frac{y + 4w}{(y + 4w)^2 + 2} . \tag{3.12}$$

One finds that $\langle \overline{\Psi}\Psi \rangle$ has a maximum on the straight line

$$y + 4w = \sqrt{2} . \tag{3.13}$$

Note that for d dimensions the number $\sqrt{2}$ in eqs. (3.11) and (3.13) would be replaced by $\sqrt{d/2}$. This is the reason why we write $\sqrt{2}$ throughout the paper. An exact expression for $\langle \overline{\Psi}\Psi \rangle$, which follows from eqs. (3.10) and (3.9), can be evaluated numerically and the position of the maximum indeed turns out to be well described by the line (3.13).

3.5. $\kappa \to -\infty$ LIMIT AT $w = 0$

This turns out to be a complicated and interesting limit. Assuming that the fluctuations of the scalar field are unimportant for large negative κ we insert $\Phi_x = (v + \varepsilon_x v_{\mathrm{st}})\mathbb{1}$ in the fermion matrix. Keeping in mind a possible presence of the FI phase, we allow $v \neq 0$.

Going over to the staggered fermion representation (2.8) and using the formalism of ref. [26] the fermion matrix in momentum space can be written as

$$A = (i\not{s} + y(v + \hat{\varepsilon} v_{\mathrm{st}}))\mathbb{1} , \tag{3.14}$$

where $\not{s} = \Gamma_\mu s_\mu (-\pi/2 < p_\mu \leqslant \pi/2)$, $\hat{\varepsilon} = \Gamma_5 \Xi_5$, and the Γ's and the Ξ's are 16-dimensional Dirac and flavour matrices. The matrix $\mathbb{1}$ in eq. (3.14) is a tensor product of unit matrices in SU(2), Dirac and "staggered" spaces.

First we calculate the eigenvalues of the fermion matrix (3.14) assuming $v = 0$ and $v_{\mathrm{st}} = 1$, which is correct at $\kappa = -\infty$ in the quenched approximation and most probably also in the unquenched model. Taking the square of A and using

$\{\Gamma_5, \Gamma_\mu\} = 0$, one easily obtains the eigenvalues

$$\begin{aligned} \mu + i\lambda &= \pm\sqrt{y^2 - s^2} \qquad |y| > |s| \\ &= \pm i\sqrt{s^2 - y^2} \qquad |y| < |s| \,. \end{aligned} \tag{3.15}$$

Thus in the thermodynamic limit there are zero eigenvalues at any y in the interval $|y| \leqslant 2$. On a finite lattice the zero eigenvalues appear only at singular y-points, which are completely determined by the possible momenta on the finite lattice, i.e. by the size, shape and boundary conditions of the lattice. Their effects in numerical simulation are violent, in particular the inversion of the fermion matrix is very difficult in the vicinity of these singular points.

Assuming that for large negative κ the fermion matrix is of the form (3.14) one can calculate $\langle \overline{\Psi}\Psi \rangle$:

$$\begin{aligned} \langle \overline{\Psi}\Psi \rangle &= \tfrac{1}{128} \mathrm{P} \int_{-\pi/2}^{\pi/2} \frac{\mathrm{d}^4 p}{\pi^4} \operatorname{Tr} A(p)^{-1} \\ &= \tfrac{1}{128} \mathrm{P} \int_{-\pi/2}^{\pi/2} \frac{\mathrm{d}^4 p}{\pi^4} \operatorname{Tr} \frac{-i\not{s} + y(v - \hat{\varepsilon} v_{\mathrm{st}})}{s^2 + y^2\left(v^2 - v_{\mathrm{st}}^2\right)} \mathbb{1} \\ &= yv \mathrm{P} \int_{-\pi/2}^{\pi/2} \frac{\mathrm{d}^4 p}{\pi^4} \frac{1}{s^2 + y^2\left(v^2 - v_{\mathrm{st}}^2\right)} \,. \end{aligned} \tag{3.16}$$

In a very similar way one can also estimate the invariant fermion condensate (2.22) when Φ_x in eq. (2.22) is replaced by $\varepsilon_x \mathbb{1}$:

$$\langle \overline{\Psi}\varepsilon\Psi \rangle = -yv_{\mathrm{st}} \mathrm{P} \int_{-\pi/2}^{\pi/2} \frac{\mathrm{d}^4 p}{\pi^4} \frac{1}{s^2 + y^2\left(v^2 - v_{\mathrm{st}}^2\right)} \,. \tag{3.17}$$

The integrals in eqs. (3.16) and (3.17) have cuts as functions of y. Taking $v = 0$ and $v_{\mathrm{st}} = 1$ in the denominators of the integrand these cuts lie in the interval $|y| \leqslant 2$. A proper definition of the integrals on the cuts would require a study of the contribution of the field fluctuations which presumably smooth the singularities. Our numerical results indicate that the fermion condensates at large negative κ stay real. We thus assume that the integrals above have to be handled by the principal value prescription.

On finite lattices the integrals (3.16) and (3.17) reduce to sums over poles. For $v = 0$ and $v_{\mathrm{st}} = 1$ the poles in y are again completely determined by the momenta possible on a particular lattice and they coincide with the y-points where the

eigenvalues (3.15) vanish:

$$\langle \bar{\Psi}\Phi\Psi \rangle = -y \sum_{p_\mu} \frac{1}{s^2 - y^2} . \tag{3.18}$$

Here the sum is taken over all momenta and s^2 is defined in eq. (3.3).

From the above considerations we conclude, assuming in the unquenched case $v \to 0$ as $\kappa \to -\infty$, that the condensates behave as

$$\begin{aligned} \langle \bar{\Psi}\Psi \rangle &\propto v \\ &= 0 \quad \text{at} \quad \kappa = -\infty , \\ \langle \bar{\Psi}\Phi\Psi \rangle &\propto v_{\mathrm{st}} \\ &\neq 0 \quad \text{at} \quad \kappa = -\infty . \end{aligned} \tag{3.19}$$

In particular, on finite lattices $\langle \bar{\Psi}\Phi\Psi \rangle$ develops poles at precisely known y-points. These poles are easily detectable in numerical simulations and can be used for tests of the code. They should not be misinterpreted as signals for phase transitions.

4. Observables with fermion fields in the quenched approximation

As discussed above, the pure Φ^4 model can be either in the symmetric PM phase or in one of the broken phases, FM or AM, where $\mathrm{SU(2)_L} \otimes \mathrm{SU(2)_R}$ is broken to its diagonal subgroup. The inclusion of fermions in the quenched approximation of course does not influence this phase structure. However, observables containing fermion fields (e.g. fermion condensates and propagators) are highly nonlocal when expressed in terms of the scalar fields after the fermionic path integration has been carried out. These observables can thus show an interesting dependence on the coupling constants and even develop singularities.

The accumulated experience with quenched and unquenched calculations in lattice theories with fermions suggests that many structures observed for observables with fermion fields in the quenched approximation have remarkably similar analogues in the unquenched cases. A systematic study of these observables in the quenched approximation can thus give hints about the phase structure of the unquenched model and elucidate the interpretation of various phases. Furthermore, in the quenched case the properties of the observables with fermion fields can be easily related to those of the scalar sector which is known in great detail [31, 34]. For these reasons we have performed in the quenched approximation a systematic investigation of the fermion condensates, of N_{CG} and in part also of the

fermion mass in the $\{\kappa, y, w\}$ coupling parameter space. Results for the eigenvalues of the fermion matrix will be reported elsewhere [33].

4.1. DETAILS ABOUT THE QUENCHED NUMERICAL SIMULATIONS

For equilibrated scalar field configurations obtained by a Hybrid Monte Carlo (HMC) algorithm for the O(4) symmetric Φ^4 theory we have performed conjugate gradient inversions on 4^4 and 6^4 lattices. On configurations separated by 100 HMC iterations we have measured the fermionic condensate $\langle\overline{\Psi}\Psi\rangle$, the invariant condensate $\langle\overline{\Psi}\Phi\Psi\rangle$ and the number N_{CG} of conjugate gradient iterations required for one inversion with fixed accuracy. The last quantity shows a sharp peak when an eigenvalue of the fermion matrix becomes very small [33]. For the measurement of $\langle\overline{\Psi}\Psi\rangle$ and $\langle\overline{\Psi}\Phi\Psi\rangle$ we apply the technique of gaussian noise. Because of the noninvariance of $\langle\overline{\Psi}\Psi\rangle$ we invert the fermion matrix for Φ field configurations rotated according to the prescription (2.19). We have performed runs at fixed values of w and κ for various values of y:

$w = 0$: $\kappa = 0.29, -0.33, -0.6, -1.2, -\infty (6^4)$

$= 0.33, 0.2, -0.5, -1.0, -1.5, -2.0, -2.5, -3.0, -6.0, -10.0, -20.0\ (4^4)$

$w = 0.2$: $\kappa = 0.29\ (6^4)$.

At each point chosen in the coupling parameter space we have typically accumulated 30–50 values for each observable. We have also varied boundary conditions for fermion fields, using completely antiperiodic, antiperiodic in one direction and sometimes, for comparison, also fully periodic boundary conditions.

In addition we have calculated the fermion mass m_{F} at $w = 0$ and $\kappa = 0.29$ in the PM phase for various values of y following the method described in refs. [16, 25]. Here we use a $6^3 12$ lattice with periodic boundary conditions in space and antiperiodic ones in time for the fermion fields. For the propagator measurement we have performed inversions of the fermion matrix for 128 Φ-field configurations separated by 100 HMC iterations in the pure O(4) model.

4.2. STRONG AND WEAK COUPLING REGIONS IN THE FM PHASE

From our earlier calculation of the fermion mass at $w = 0$ in the quenched approximation it has become evident that the FM phase of our model has two regions, a "weak" and a "strong" coupling region, FM(W) and FM(S), where the fermion masses decrease or increase, respectively, as $\kappa \searrow \kappa_{\mathrm{c}}$ at a fixed y [16]. Thus the two regions are separated by a crossover at $y \approx \sqrt{2}$ (see figs. 1 and 2 in ref. [16]), where the dependence of the fermion mass on κ changes, and $\langle\overline{\Psi}\Psi\rangle$ has a peak. The peak height decreases with decreasing κ. The crossover is indicated in fig. 2 by the dotted vertical line.

Recently, $\langle \overline{\Psi}\Psi \rangle$ and the fermion and the doubler masses have also been calculated for $w > 0$ in the quenched approximation [12, 25]. The picture which has emerged is that with increasing w the strong coupling region FM(S) expands to smaller y values. The crossover region is found at $y + 4w \approx \sqrt{2}$. For $w > \sqrt{2}/4$, only the FM(S) region is found at positive y (see fig. 2 of ref. [25]).

In the FM phase we could not detect any dependence of the position of the crossover on κ. We have checked that the peak of $\langle \overline{\Psi}\Psi \rangle$ does not develop into a singularity as the lattice size increases. Nevertheless, the number of conjugate gradient iterations N_{CG} increases significantly at the crossover. We show N_{CG} as a function of y for $\kappa = 0.33$ in fig. 3. Actually the easiest way to localize the crossover is to look for the peak in N_{CG}.

4.3. SPLITTING OF THE PM PHASE

In the PM phase the noninvariant observables $\langle \Phi \rangle$, $\langle \overline{\Psi}\Psi \rangle$ and $\langle \Phi_{st} \rangle$ vanish. However, $\langle \overline{\Psi}\Phi\Psi \rangle$, N_{CG} and the fermion mass show y-dependent structures. We shall describe them first for $w = 0$.

The observable $\langle \overline{\Psi}\Phi\Psi \rangle$ is close to zero at $y < \sqrt{2}$, increases steeply around $y \approx \sqrt{2}$ and stays distinctly nonzero at larger y, decreasing as $1/y$ for large y. In the PM phase the invariant condensate thus behaves like an order parameter distinguishing between different phases. As this is also true in the unquenched case, we call, even in the quenched approximation, the regions of the PM phase to the left and right of $y \approx \sqrt{2}$ the PMW and PMS phases, respectively. However, we continue to call the boundary between them a crossover (in the infinite volume limit it is probably a singularity of nonlocal bosonic observables). In the unquenched case it does not correspond to a single phase transition line but develops into the funnel-like structure partly filled with the FI phase.

In fig. 3 we show N_{CG} at $w = 0$ and $\kappa = 0.20$ on a 4^4 lattice. A pronounced symmetric peak, much higher than in the FM phase, is present around the crossover. With decreasing κ the peak in N_{CG} stays at the same y but increases in height. A recent study of the fermion matrix shows that the peak is caused by some of its eigenvalues approaching zero at $y \approx \sqrt{2}$ [33].

In fig. 4 we display our results for the fermion mass m_F at $\kappa = 0.29$ with $w = 0$ on the $6^3 12$ lattice. In the PMW phase m_F is consistent with zero. At $y \approx \sqrt{2}$ the mass grows rapidly with y. The present data do not allow us to decide on whether m_F jumps or whether it rises continuously. Above the crossover m_F increases roughly linearly with y. The slope of the increase is consistent with the expected value z^{-1}. For comparison we include a dashed line of this slope in fig. 4. Thus, the crossover detected already in the FM phase also continues in the PM phase and divides that phase into a massless weak Yukawa coupling phase PMW and a massive strong Yukawa coupling phase PMS.

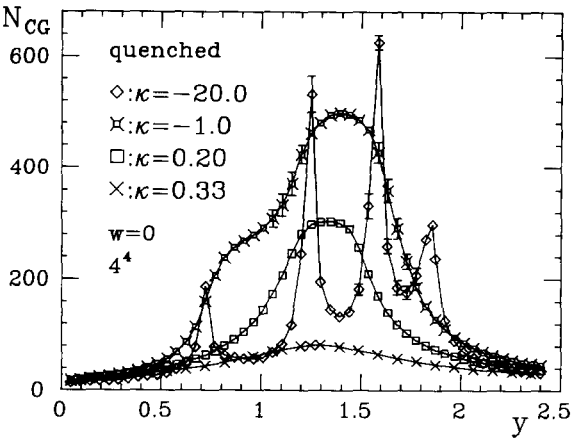

Fig. 3. The number of conjugate gradient iterations as a function of y for several values of κ in the quenched model. The sharp peaks at $\kappa = -20.0$ are at the positions given by eq. (4.1). Error bars smaller than twice the size of the symbols are dropped for clarity.

The runs performed at $w = 0.2$ and $\kappa = 0.29$ show that the crossover in the PM phase is shifted along the line (3.13) to a smaller value of y. We assume this to be true in the whole PM phase.

4.4. SINGULARITIES IN THE AM PHASE

The singularity structure of the observables with fermion fields deep in the AM phase is unusual. We have restricted its investigation mostly to the $w = 0$ case. On

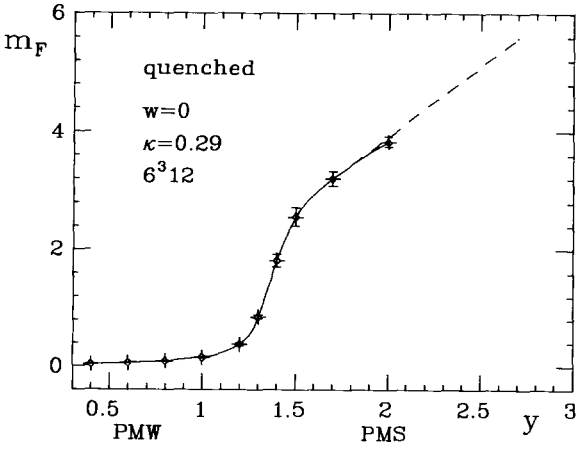

Fig. 4. The fermion mass m_F in the quenched approximation at $w = 0$ as a function of y for $\kappa = 0.29$, i.e. in the PM phase.

one hand, for κ not far below the PM–AM phase transition line at $\kappa = -\kappa_c$, the crossover line from the PM phase seems to continue. This is best seen in the observable N_{CG}. As seen in fig. 3, for $\kappa = -1.0$ it still has a maximum around $y \approx \sqrt{2}$, much higher than in the PM phase. The crossover is indicated in fig. 2 by the dashed line. It splits the AM phase into the AM(W) and AM(S) regions.

On the other hand, at $\kappa = -\infty$ we expect, at least for $w = 0$, the lattice-size dependent singularities described in subsect. 3.5. We have calculated the fermionic condensates on several finite lattices with various boundary conditions using the fully antiferromagnetic field configuration $\Phi_x = \varepsilon_x \mathbb{1}$, which corresponds to a quenched simulation at $\kappa = -\infty$. We have found at the right places several sharp peaks in N_{CG}, arising from the vanishing eigenvalues (3.15), and poles in $\langle \bar{\Psi} \Phi \Psi \rangle$, in agreement with the relation (3.18). For example, on a 4^4 lattice with antiperiodic boundary conditions in one direction for the fermions the positions are

$$y \approx 0.71,\ 1.22,\ 1.58 \text{ and } 1.87. \tag{4.1}$$

At these positions we have also found some bumps in $\langle \bar{\Psi} \Psi \rangle$, which should, according to eq. (3.16), actually vanish. This can supposedly be explained by the unreliability of the fermion matrix inversion at these special y values.

This structure also manifests itself at finite but large negative κ. This is seen for N_{CG} at $\kappa = -20.0$ in fig. 3 and for $\langle \bar{\Psi} \Phi \Psi \rangle$ at $\kappa = -10.0$ in fig. 5a. The peaks in $\langle \bar{\Psi} \Phi \Psi \rangle$ are even more pronounced at $\kappa = -20.0$. As seen in fig. 3, N_{CG} develops, already at $\kappa = -1.0$, a shoulder on the left-hand side. Decreasing κ more and

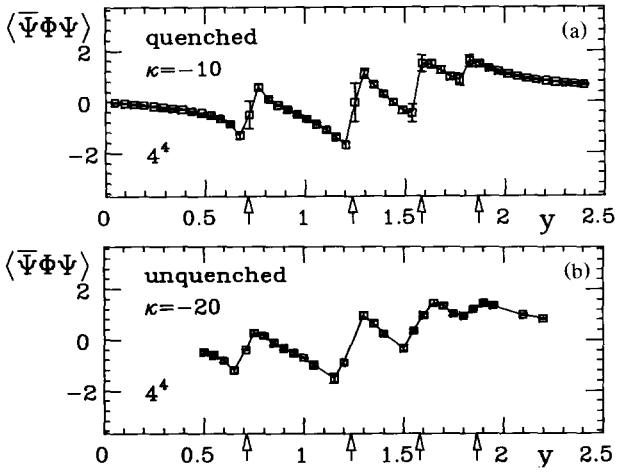

Fig. 5. The invariant condensate $\langle \bar{\Psi} \Phi \Psi \rangle$ as a function of y for (a) $\kappa = -10.0$ in the quenched and (b) $\kappa = -20.0$ in the unquenched case. The vertical arrows indicate the expected positions (4.1) of the poles at $\kappa = -\infty$.

more the asymmetry of such curves becomes more pronounced and at $\kappa = -20.0$ the curve splits into sharp peaks at the expected y values.

For $w > 0$ we expect the crossover to shift in a similar way as in the FM and PM phases. At $\kappa = -\infty$ with $w > 0$ we have found an even richer pole structure than at $w = 0$.

5. Phase diagram of the model with dynamical fermions

As mentioned earlier, the determinant of the fermion matrix of the investigated model is real. This enables us to use the Hybrid Monte Carlo (HMC) algorithm for a simulation of the full model with two identical doublets of dynamical fermions. The resulting phase diagram is already shown in fig. 1 for the $w = 0$ case. For $w > 0$ there seems to be essentially a shift of this phase diagram in the negative y direction so that the new phase diagram for fixed w is still given approximately by a part of fig. 1 with the zero of the new y coupling axis shifted to $y = 4w$.

5.1. DETAILS ABOUT THE UNQUENCHED SIMULATIONS

Using mostly a 6^4 lattice we have monitored all the observables described in subsect. 2.2 in the three-dimensional parameter space $\{\kappa, y, w\}$. Each observable is calculated from at least 100 Monte Carlo configurations. In a HMC trajectory we have usually chosen the step-size $\Delta\tau$ and the number of steps N such that the product $N\Delta\tau = 1$. Only at very negative values of κ where $\Delta\tau$ had to be reduced, was the product chosen smaller than unity to have reasonable Metropolis accep-

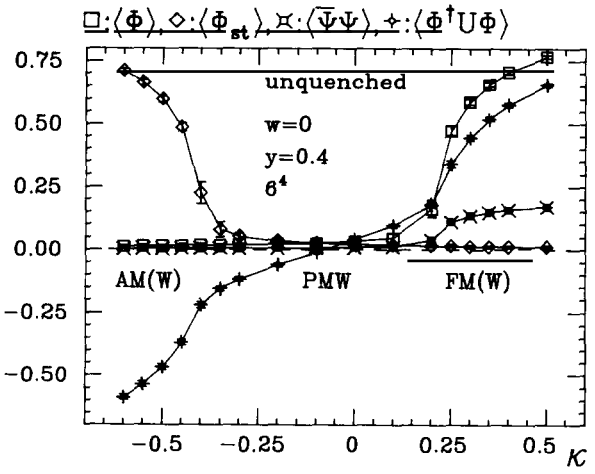

Fig. 6. The observables $\langle\Phi\rangle$, $\langle\Phi_{st}\rangle$, $\langle\bar{\Psi}\Psi\rangle$ and $\langle\Phi^{\dagger}U\Phi\rangle$ as functions of κ for $y = 0.4$ and $w = 0$, i.e. in the weak coupling regions in the unquenched model.

tance at the end of the trajectory. In these cases we have always performed more HMC sweeps in between measurements. We have mostly used periodic boundary conditions in all directions except for an antiperiodic condition in one direction for the fermion fields. By sometimes varying boundary conditions we wanted to get a rough idea about the finite size effects. We have found that there are appreciable finite size effects at small y and one has to be extremely careful in choosing a boundary condition there. For example, the PMW phase could hardly be seen with completely periodic boundary conditions for all fields. For large y no significant finite size effects have been observed, however.

The coupling parameter space has been scanned in the κ direction from $+0.9$ to -1.6 mostly in steps $\Delta\kappa = 0.1$ and in steps $\Delta\kappa = 0.05$ in the vicinity of the phase transition lines. We have chosen the following fixed values of w and y:

$w = 0$, $\quad y = 0.2, 0.4, 0.8, 0.9, 1.0, 1.2, 1.5, 1.7, 2.0, 2.4, 3.0, 4.0, 7.0, 10.0, 20.0$.

$w = 0.5$, $\quad y = 0.3, 1.0, 2.0, 3.0$.

The coupling parameter space has also been scanned in the y direction in the interval $y = 0.2$–10.0 in steps $\Delta y = 0.05$–0.2 for the following fixed values of w and κ:

$w = 0$, $\quad \kappa = 4.0, 0.0, -1.0, -1.6, -2.6, -4.0, -10.0, -20.0$.

$w = 0.2$, $\quad \kappa = 0.0, -1.6$.

$w = 0.5$, $\quad \kappa = 0.0, -1.6$.

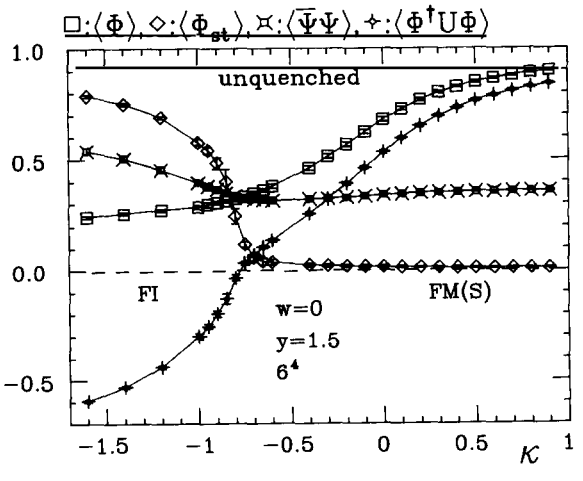

Fig. 7. Same as in fig. 6 for $y = 1.5$, i.e. close to the crossover in the FM and FI phases in the unquenched model.

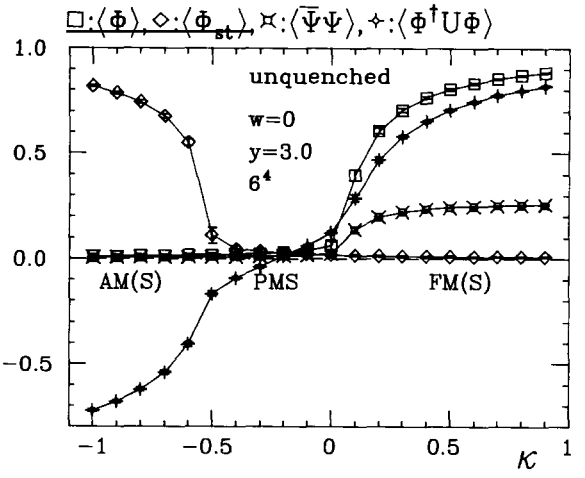

Fig. 8. Same as in fig. 6 for $y = 3.0$, i.e. in the strong coupling regions in the unquenched model.

5.2. PHASES AT $w = 0$

In the following we describe the properties of the different phases in terms of the observables we have measured. For interpretation of the phases and regions we also use their correspondence to the similar regions in the quenched case where some additional results are available. Examples of our results for $w = 0$ can be found in a number of figures: figs. 6, 7 and 8 show $\langle \Phi \rangle$, $\langle \Phi_{st} \rangle$, $\langle \bar{\Psi}\Psi \rangle$ and $\langle \Phi^\dagger U \Phi \rangle$ in scans along the κ direction at fixed values of $y = 0.4$ (weak), 1.5

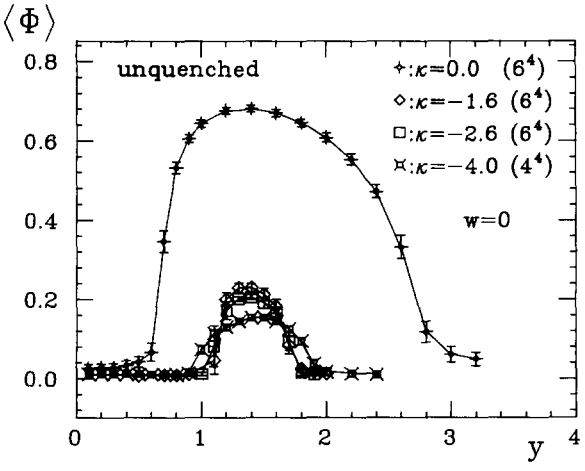

Fig. 9. The magnetization $\langle \Phi \rangle$ as a function of y for several fixed κ values in the unquenched model with $w = 0$. For clarity, only the error bars larger than the size of the symbols are shown.

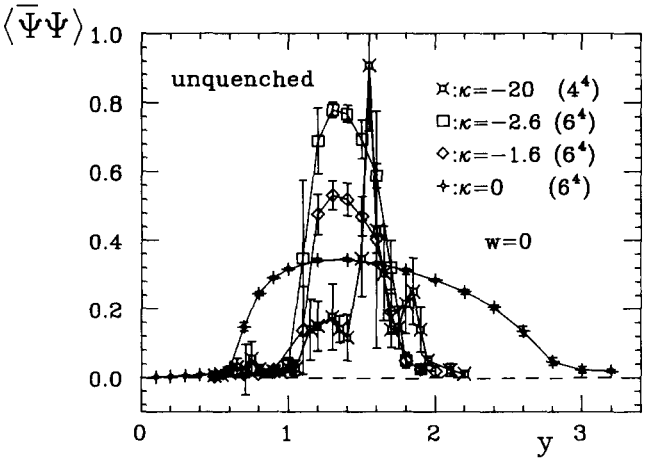

Fig. 10. The condensate $\langle \bar{\Psi}\Psi \rangle$ as a function of y for several fixed κ values in the unquenched model with $w = 0$.

(intermediate) and 3.0 (strong), respectively. These figures show the most interesting observables in all the phases. Figs. 9, 10 and 11 illustrate in more detail the funnel-like structure in scans along the y direction at fixed values of $\kappa = 0.0, -1.6, -2.6, -4.0$ with $w = 0$.

FM: In this phase $\langle \Phi \rangle \neq 0$, $\langle \bar{\Psi}\Psi \rangle \neq 0$, $\langle \bar{\Psi}\Phi\Psi \rangle \neq 0$ and $\langle \Phi_{st} \rangle = 0$ (figs. 6–8). $\langle \Phi^\dagger U \Phi \rangle$ is always positive here. Similar to the quenched model [16, 25], the FM phase is divided into two regions by a crossover at $y + 4w \approx \sqrt{2}$. Some preliminary unquenched calculations of the fermion mass also indicate that at lower y values, i.e. in the FM(W) region, the fermion mass decreases with decreasing v. On the contrary, at larger y values, i.e. in the FM(S) region, the fermion mass increases as v decreases at a fixed y. The precise position of the crossover (the dotted line in fig. 1) in the FM phase with respect to the points A, B is under investigation.

PMW: This phase is characterized by $\langle \Phi \rangle = 0$, $\langle \bar{\Psi}\Psi \rangle = 0$ and $\langle \Phi_{st} \rangle = 0$ (fig. 6). The value of $\langle \bar{\Psi}\Phi\Psi \rangle$ is very small and it changes sign as κ is lowered somewhere in the middle of this phase, at the same place where $\langle \Phi^\dagger U \Phi \rangle$ (fig. 6) changes sign too. Following the correspondence with the quenched results (fig. 4), in this phase we expect massless fermions.

PMS: In terms of the order parameters $\langle \Phi \rangle$, $\langle \bar{\Psi}\Psi \rangle$ and $\langle \Phi_{st} \rangle$ this phase is like the PMW phase (fig. 8). However, it is completely separated from the PMW phase by the upper part of the funnel containing the FM phase. As in the quenched case (fig. 4), we anticipate massive fermions in this phase. Unlike in the PMW phase, the value of $\langle \bar{\Psi}\Phi\Psi \rangle$ is appreciable.

AM: Here $\langle \Phi \rangle = 0$, $\langle \bar{\Psi}\Psi \rangle = 0$, but $\langle \Phi_{st} \rangle \neq 0$ (figs. 6, 8). The value of $\langle \Phi^\dagger U \Phi \rangle$ is negative. The funnel with the FI phase separates the AM phase into the AM(W)

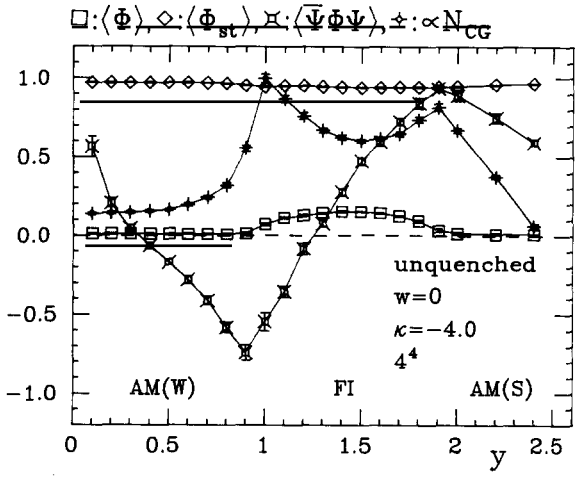

Fig. 11. The observables $\langle \Phi \rangle$, $\langle \Phi_{st} \rangle$, $\langle \bar{\Psi} \Phi \Psi \rangle$ and N_{CG} as functions of y at $\kappa = -4.0$ in the unquenched model with $w = 0$.

and AM(S) regions. Because the funnel possibly stops at large negative but finite κ (see discussion below), these regions could very well be connected.

FI: This is a phase with both ferromagnetic and antiferromagnetic ordering of the scalar field, i.e. $\langle \Phi \rangle \neq 0$ and $\langle \Phi_{st} \rangle \neq 0$ (figs. 7, 9, 11). We have also found that $\langle \bar{\Psi} \Psi \rangle$ is nonvanishing in the FI phase and has a peak as a function of y around $y \approx \sqrt{2}$ (fig. 10). Furthermore, N_{CG} and the fluctuations of $\langle \bar{\Psi} \Psi \rangle$ go up quite substantially at the AM(W)–FI and FI–AM(S) phase boundaries (figs. 10, 11). If at a fixed value of κ a scan is made in the y direction, $\langle \bar{\Psi} \Phi \Psi \rangle$ falls to a large negative value at the AM(W)–FI phase boundary, then grows from this large negative value to a large positive value in the FI phase and finally drops to a small positive value in the AM(S) region (fig. 11). While scanning the FI phase in the other direction, varying κ with a fixed y (fig. 7), we have observed a monotonic decrease of $\langle \Phi \rangle$ (see also fig. 9) and a monotonic increase of $\langle \Phi_{st} \rangle$. We have found at $\kappa = -10.0$ a still significantly nonvanishing, though tiny value (about 0.03) of $\langle \Phi \rangle$ around $y \approx \sqrt{2}$. At $\kappa = -20.0$ the signal seems to be consistent with zero within our accuracy.

This brings us to the question of the behaviour of the model and of the fate of the funnel with the FI phase at large negative κ. Does the funnel continue to $\kappa = -\infty$, separating completely the AM(W) and AM(S) regions, or does $\langle \Phi \rangle$ vanish below some large negative but finite κ? A competition of the anti-ordering tendency of the hopping term and of the ordering tendency of the Yukawa coupling apparently inhibits the onset of some asymptotic behaviour at moderate negative values of κ. But at large negative κ, as in the quenched case, the poles in eq. (3.18) and the peaks in N_{CG} expected on finite lattices at $\kappa = -\infty$ already show up, making precise calculation, e.g. of $\langle \Phi \rangle$ practically impossible.

Fig. 5b displays $\langle \bar{\Psi}\Phi\Psi \rangle$ at $\kappa = -20.0$. Comparing figs. 5a and 5b we conclude that in the unquenched case the poles develop later than in the quenched approximation (the strikingly similar curves have been obtained for $\kappa = -10.0$ in the quenched case and for $\kappa = -20.0$ in the unquenched case), but they are of the same character, in accordance with the expectation that $\Phi_x = \varepsilon_x \mathbb{1}$ at $\kappa = -\infty$ also in the unquenched model. Thus at $\kappa = -\infty$ the quenched approximation is possibly exact and for dynamical fermions the antiferromagnetic ordering of the hopping term wins completely over the ferromagnetic ordering by the Yukawa term.

The strong singularities indicate that the conjugate gradient inversion gets unreliable, as observed already in the quenched case (fig. 3), possibly causing spurious results. We think that one of such unreliable results might be the signal for $\langle \bar{\Psi}\Psi \rangle$ at $\kappa = -20.0$, shown in fig. 10. According to eq. (3.16) this observable is actually expected to vanish as $v \to 0$. Figs. 7 and 10 show that in the interval of κ from 0 to -2.6 the condensate $\langle \bar{\Psi}\Psi \rangle$ still increases while v decreases. This is another indication that the asymptotic behaviour sets in probably only at large negative κ.

Being thus unable to trace the funnel containing the FI phase at large negative κ we can only guess on the basis of our results at $\kappa = -20.0$ that the funnel presumably ends at some finite κ and the AM(W) and AM(S) regions are connected around it. Of course it is also not excluded by our data that the funnel continues down to $\kappa = -\infty$.

5.3. THE $w > 0$ CASE

Fig. 12 shows $\langle \bar{\Psi}\Psi \rangle$ versus y at $\kappa = 0$ for fixed values of $w = 0.0, 0.2, 0.5$. The curves are almost identical to one another except that with increasing w the curves

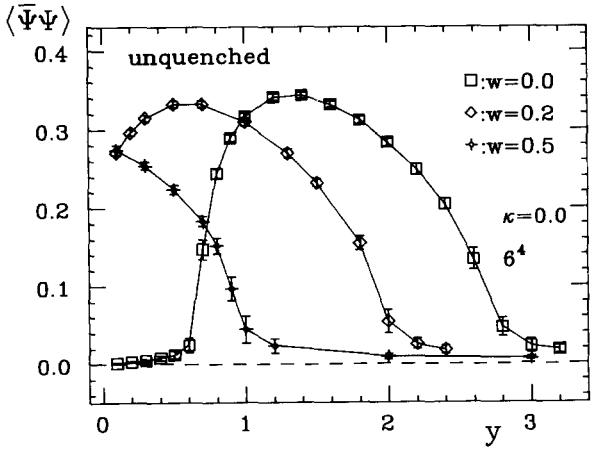

Fig. 12. The condensate $\langle \bar{\Psi}\Psi \rangle$ as a function of y at $\kappa = 0$ for several fixed values of w in the unquenched model.

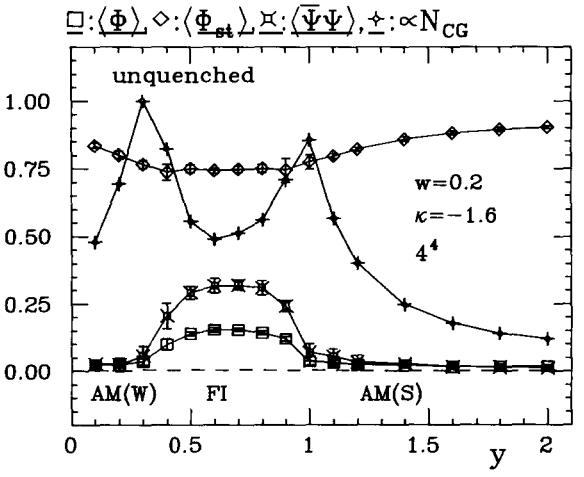

Fig. 13. The observables $\langle \Phi \rangle$, $\langle \Phi_{st} \rangle$, $\langle \bar{\Psi}\Psi \rangle$ and N_{CG} as functions of y at $\kappa = -1.6$ in the unquenched model with $w = 0.2$.

shift to the left along the lines $y + 4w = \text{const.}$, as observed also in the quenched case. The curves for $\langle \Phi \rangle$ are very similar.

The funnel in the negative κ region shifts in the same way, as depicted in fig. 13 at $w = 0.2$ and $\kappa = -1.6$. We also have evidence from the runs in the κ direction at different fixed values of y and $w = 0.5$ that the FM(S) and AM(S) regions as well as the PMS phase appear at the expected places after the origin of y in fig. 1 is shifted to 2.0 ($= 4w$).

All the accumulated evidence seems to be consistent with the above discussed shift along the $y + 4w = \text{const.}$ lines, though, of course, the scan of the phase diagram with $w > 0$ is not complete, especially in the funnel region. In particular,

TABLE 1
Some points of the FM(S)–PMS and PMS–AM(S) phase transition lines at $w = 0.5$ on a 6^4 lattice

FM(S)–PMS		PMS–AM(S)	
y	κ	y	κ
0.5	-0.22 ± 0.08	1.0	-0.55 ± 0.05
0.8	-0.05 ± 0.05	2.0	-0.45 ± 0.05
1.0	-0.05 ± 0.05	3.0	-0.40 ± 0.05
1.0 ± 0.2	0.00		
2.0	0.15 ± 0.05		
3.0	0.25 ± 0.05		

we do not yet know the position of the crossover in the FM phase with respect to the lines A, B. For future mass calculations in the FM(S) and PMS phases and a study of the decoupling of the doublers it is important to locate rather precisely the FM(S)–PMS and PMS–AM(S) phase transition lines for w sufficiently large such that the line $y = 0$ falls in the strong coupling region. Then the physical fermion mass can remain small as seen in the quenched approximation in ref. [25]. We give in table 1 some positions of these lines for $w = 0.5$.

6. Conclusion and outlook

The phase structure of the chiral $SU(2)_L \otimes SU(2)_R$ scalar-fermion model turns out to be very complex. Assuming that the funnel containing the FI phase does not continue to $\kappa = -\infty$, the model has for $y \geqslant 0$, $w \geqslant 0$ and arbitrary real κ seven distinct regions lying in five phases. The phases are separated by six different phase transition sheets. Within our accuracy of their location, the phase transitions meet for $w = 0$ at two quadruple points A, B, which for $w > 0$ presumably continue as lines A, B in the three-dimensional space of coupling parameters. At present we have little information about the order of the transitions in the model except that we have nowhere observed phenomena indicating a strong first order. In addition, in consequence of the theorem in ref. [28] that the fermion mass vanishes at $y = 0$ for any w, the fermionic correlation length diverges everywhere on the sheet $y = 0$.

The dynamics of fermions has a strong feedback on the scalar sector for intermediate values of the Yukawa couplings and tends to align the scalar field. The FM phase extends to the negative κ region and splits the PM phase in two different phases, PMW and PMS with massless and massive fermions, respectively. For negative κ the FM phase ends at the phase transition to the FI phase which still has ferromagnetic properties mixed up with antiferromagnetic ones. Also, the antiferromagnetic phase is split over a large κ range into two regions AM(W) and AM(S).

We show that with the exception of the FI phase all the phases and their regions found in the unquenched model have corresponding analogues in the quenched model. This is of help for the interpretation of the various phases and regions, as in the quenched case the calculations are easier and quite a lot of information about the fermion and the doubler masses is available.

Some of the regions are surely not relevant for the standard model but could be useful in other branches of physics. Concerning the standard model or, in general, the electroweak interactions, we would like to mention some points of interest:

(i) The FM(S) region in the neighbourhood of the FM(S)–PMS phase transition with $w \geqslant 0.5$ and small values of y appears to be very promising for the decoupling of the fermion doublers [25]. The fermion mass can be kept small in the scaling region by taking y close to 0 whereas the doubler masses are expected to stay of

the order of cutoff without tuning w. Our quenched results [12, 25] support these expectations. Further investigation is necessary to check that the perturbative properties of the standard model are reproduced in this region.

(ii) In the FM(W) region fermion doubling occurs. However, it may be possible that tuning both y and w toward the line A raises the doubler masses sufficiently such that the low-energy phenomenology is practically unaffected. In the quenched approximation the crossover intersects the FM–PM transition line, which appears to offer the possibility of decoupling the fermion doublers in the FM(W) scaling region at small y by tuning w toward the intersection point [6, 12, 25]. Whether such a decoupling is really possible depends crucially on the position of the crossover with respect to the line A in the full model with dynamical fermions.

(iii) The PMS phase containing, for small y and sufficiently large w, massive fermions and heavy doublers in spite of $v = 0$, could be of interest for more general field-theoretical investigations, e.g. for the asymptotically free chiral gauge theories without scalar fields in the classical action [6, 19].

(iv) It could also be that the model possesses nontrivial fixed points on the lines A, B where an interesting field theory is obtained in the continuum limit.

The exploration of the phase structure done in this work is a necessary prerequisite for the studies of these interesting questions which we want to address in the future.

We have benefitted from discussions with I.M. Barbour, A. Hasenfratz, C.B. Lang, J. Shigemitsu and R.E. Shrock. The continuous support by H.A. Kastrup is gratefully acknowledged. The computations were performed on the CRAY Y-MP/832 at HLRZ Jülich.

Note added in proof

(1) Recently the possibility of decoupling the doublers in the FM(S) region of our model has been demonstrated also in the unquenched calculation [36].

(2) In a recent paper [37] the decoupling of the fermion doublers was found possible also in a class of fermion-scalar models with Wilson–Yukawa coupling which were formulated in the spirit of refs. [5, 38, 39] and happen to lack the Golterman–Petcher (GP) symmetry [28]. We expect that the type of models in ref. [37] are not essentially different from our's (i.e. will be in the same universality class), but welcome in our model the GP symmetry which is of course very helpful in pinning down the critical Yukawa coupling.

We would like to comment on some remarks in that paper: One may get the impression from ref. [37] that our fermion-scalar model applies only to right handed fermions with hypercharge zero. This is not the case. The lattice formulation [21–23] of the standard model has a straightforward reduction (i.e. leaving out gauge fields and considering only mass degenerate doublets) to our SU(2) ⊗ SU(2)

fermion-scalar model. Our model therefore applies to fermions in all weak hypercharge representations occurring in the standard model. The decoupling of doublers found in refs. [25,36] is thus relevant for all fermions in the standard model in the weak gauge coupling limit.

(3) We have learned from M.A. Stephanov and M.M. Tsypin [40] that they have found in their mean field calculations [17] extended to the SU(2) ⊗ SU(2) case an indication of the crossings of the FM(W)–PMW and AM(W)–PMW lines (our point A) and of the FM(S)–PMS and AM(S)–PMS lines (point B). We thank these authors for their information and also for pointing out to us an erroneous factor in our MF calculations, which however does not change our failure to find there the points A and B.

References

[1] P. Hasenfratz, Nucl. Phys. B (Proc. Suppl.) 9 (1988) 3
[2] J. Jersák, *in* Higgs particle(s) – Physics issues and searches in high energy collisions (Erice Workshop, July 1989), ed. A. Ali (Plenum, New York) to be published;
A. Hasenfratz, preprint AZPH-TH/89-75
[3] L.H. Karsten and J. Smit, Nucl. Phys. B183 (1981) 103;
H. Nielsen and M. Ninomiya, Nucl. Phys. B185 (1981) 20
[4] K.G. Wilson, *in* New phenomena in subnuclear physics, ed. A. Zichichi (Plenum, New York, 1977) p. 69
[5] J. Smit, Nucl. Phys. B (Proc. Suppl.) 4 (1988) 451
[6] J. Smit, Nucl. Phys. B (Proc. Suppl.) 17 (1990)
[7] J. Kuti, Nucl. Phys. B (Proc. Suppl.) 9 (1989) 55;
H. Neuberger, Nucl. Phys. B (Proc. Suppl.) 17 (1990)
[8] J. Shigemitsu, Phys. Lett. B189 (1987) 164, OSU preprint DOE/ER/01545-397 (unpublished);
A.M. Thornton, Phys. Lett. B214 (1988) 577;
J. Kuti, Nucl. Phys. B (Proc. Suppl.) 17 (1990)
[9] J. Polonyi and J. Shigemitsu, Phys. Rev. D38 (1988) 3231;
D. Stephenson and A.M. Thornton, Phys. Lett. B212 (1988) 479;
J. Shigemitsu, Phys. Lett B226 (1989) 364; Nucl. Phys. B (Proc. Suppl.) 9 (1989) 96;
Y. Shen, J. Kuti, L. Lin and P. Rossi, Nucl. Phys. B (Proc. Suppl.) 9 (1989) 99
[10] A. Hasenfratz, W. Liu and T. Neuhaus, Phys. Lett. B236 (1990) 339;
A. Hasenfratz, Nucl. Phys. B (Proc. Suppl.) 17 (1990)
[11] J. Shigemitsu, Nucl. Phys. B (Proc. Suppl.) 17 (1990)
R.E. Shrock, Nucl. Phys. B (Proc. Suppl.) 17 (1990)
[12] A.K. De, Nucl. Phys. B (Proc. Suppl.) 17 (1990)
[13] I-H. Lee, J. Shigemitsu and R.E. Shrock, Nucl. Phys. B330 (1990) 225
[14] I-H. Lee, J. Shigemitsu and R.E. Shrock, Nucl. Phys. B334 (1990) 265
[15] A. Hasenfratz and T. Neuhaus, Phys. Lett. B220 (1989) 435;
A. Hasenfratz, *in* Lattice Higgs Workshop, ed. B. Berg et al. (World Scientific, Singapore, 1988) p. 229;
A. Hasenfratz, Nucl. Phys. B (Proc. Suppl.) 9 (1989) 92
[16] W. Bock, A.K. De, K. Jansen, J. Jersák and T. Neuhaus, Phys. Lett. B231 (1989) 283
[17] M.A. Stephanov and M.M. Tsypin, Phys. Lett. B236 (1990) 344, Phys. Lett. B242 (1990) 432;
M.F.L. Golterman and D.N. Petcher, preprint UCLA/90/TEP/19
[18] I. Bender, R. Horsley and W. Wetzel, preprint HD-THEP-90-03
[19] J. Smit, Nucl. Phys. B (Proc. Suppl.) 9 (1989) 579

[20] I. Montvay, Phys. Lett. B199 (1987) 89, B205 (1988) 315;
A. Borrelli, L. Maiani, G.C. Rossi, R. Sisto and M. Testa, Phys. Lett. B221 (1989) 360, Nucl. Phys. B333 (1990) 335
[21] J. Smit, Nucl. Phys. B175 (1980) 307;
L.H. Karsten, *in* Field Theoretical Methods in Particle Physics, ed. W. Rühl (Plenum, New York, 1980) 235
[22] J. Smit, Acta Physica Polonica B17 (1986) 531
[23] P.D.V. Swift, Phys. Lett. B145 (1984) 256
[24] A.M. Thornton, Phys. Lett. B221 (1989) 151, B227 (1989) 434
[25] W. Bock, A.K. De, K. Jansen, J. Jersák, T. Neuhaus and J. Smit, Phys. Lett. B232 (1989) 486
[26] M.F.L. Golterman and J. Smit, Nucl. Phys. B245 (1984) 61
[27] N. Kawamoto and J. Smit, Nucl. Phys. B192 (1981) 100
[28] M.F.L. Golterman and D.N. Petcher, Phys. Lett. B225 (1989) 159;
M.F.L. Golterman, Nucl. Phys. B (Proc. Suppl.) 17 (1990);
D.N. Petcher, Capri Conf., Nucl. Phys. B (Proc. Suppl.) 17 (1990)
[29] S. Duane, A.D. Kennedy, B. Pendelton and D. Roweth, Phys. Lett. B195 (1987) 216
[30] E. Witten, Phys. Lett. B117 (1982) 324
[31] A. Hasenfratz, K. Jansen, C.B. Lang, T. Neuhaus and H. Yoneyama, Phys. Lett. B199 (1987) 531; J. Kuti, L. Lin and Y. Shen, Phys. Rev. Lett. 61 (1988);
A. Hasenfratz, K. Jansen, J. Jersák, C.B. Lang, T. Neuhaus and H. Yoneyama, Nucl. Phys. B317 (1989) 81
[32] A. Hasenfratz, K. Jansen, J. Jersák, C.B. Lang, H. Leutwyler and T. Neuhaus, Z. Phys. C46 (1990) 257
A. Hasenfratz, K. Jansen, J. Jersák, H.A. Kastrup, C.B. Lang, H. Leutwyler and T. Neuhaus, preprint HLRZ 90-09
[33] I.M. Barbour, W. Bock, C.T.H. Davies, A.K. De, D. Henty, J. Smit and T. Trappenberg, preprint HLRZ 90-42
[34] M. Lüscher and P. Weisz, Nucl. Phys. B318 (1989) 705
[35] S. Aoki, I-H. Lee, D. Mustaki, J. Shigemitsu and R.E. Shrock, preprint ITP-SB-89-93
[36] W. Bock A.K. De, preprint HLRZ 90-29, Phys. Lett. B, to be published
[37] A. Aoki, I.-H. Lee, J. Shigemitsu and R.E. Shrock, Phys. Lett. B243 (1990) 403
[38] S. Aoki, Phys. Rev. Lett. 60 (1988) 2109; Phys. Rev. D38 (1988) 618; Nucl. Phys. B (Proc. Suppl.) 4 (1988) 479; 9 (1989) 584; Phys. Rev. D40 (1989) 2729
[39] K. Funakubo and R. Kashiwa, Phys. Rev. Lett 60 (1988) 2113; Phys. Rev. D38 (1988) 2602
[40] M.A. Stephanov and M.M. Tsypin, private communication and to be published